STATUS OF C3MJ+ AND C4MJ PRODUCTION CONCENTRATOR SOLAR CELLS AT SPECTROLAB

J.H. Ermer[1], R.K. Jones[1], P.Hebert[1], P.Pien[1] , R.R. King[1], D. Bhusari[1], R. Brandt[1]
O.Al-Taher[1], C.Fetzer, [1]G. S. Kinsey[2], and N. Karam[1]

[1]Spectrolab, Inc., USA; [2]Amonix, Inc. USA

ABSTRACT

Multijunction solar cells based on III-V semiconductors, having recently demonstrated 43.5% [1] remain the world's most efficient solar cells, and the preferred technology in point-focus and dense-array CPV system architectures. 2011 is proving to be a pivotal year for CPV technology, with multiple power plant installations in the megawatt to 10's of megawatt scale. Spectrolab is working closely with CPV system manufacturers to provide a reliable and well-characterized cell technology, in volumes commensurate with this increasing demand. The evolutionary C3MJ+ and the C4MJ cell technologies are the latest in a sequence of CPV solar cell designs, with conversion efficiencies approaching or greater than 40%. Both technologies have completed detailed characterization and qualification programs, including accelerated laboratory and (for C4MJ) on-sun reliability testing, and have entered into high volume production at Spectrolab's manufacturing facility in Sylmar, CA. The metamorphic C4MJ technology affords new opportunities to optimize cell designs taking into consideration both the spectral optical transmittance of a particular CPV system and the installation site's average solar resource over a typical meteorological year (TMY).

INTRODUCTION

Spectrolab's III-V multijunction cell technology has made steady progress through a combination of internal R&D and capital investments as well as support from the US Department of Energy's Technology Pathway Partnerships. A review of delivered efficiency of C1MJ, C2MJ, and C3MJ prior cell generations, supporting megawatts of on-sun CPV installations, shows a trend to both higher cell efficiencies and tighter production distributions (see Fig. 1).

In November 2010, Spectrolab introduced the C3MJ+ cell technology as an improved version of the C3MJ design. The improved cell is considered an evolutionary design change from the prior C3MJ cell generation since it shares an identical epitaxial structure, and incorporates only minor changes to the wafer processing sequence. Based on this close heritage, the qualification and characterization of the C3MJ+ has been established largely by similarity and is documented in the previously released C3MJ qualification report.

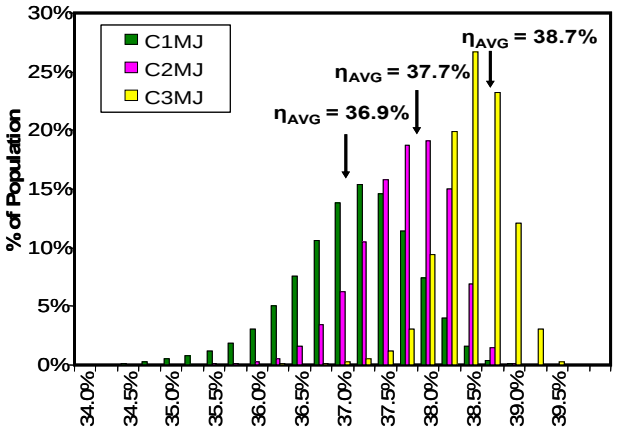

Figure 1. Production distributions for C1, C2, and C3MJ cell technology (millions of cells).

The C4MJ technology, being the first instance of a production multijunction cell with a metamorphic epitaxial design, is a more disruptive change, and the subject of a more comprehensive qualification and characterization study that will be discussed further in this paper. Details of the C4MJ's unique metamorphic epitaxial design have been discussed elsewhere [2-4].

Wafer process improvements that reduce series resistance and reflective losses through improved grid and bus bar design are identical in both the C3MJ+ and C4MJ cell designs. The new cell designs are also available with an optional gold capping layer, which overlays the standard silver contacts.

C3MJ+ and C4MJ DISTRIBUTIONS

Production builds of the improved C3MJ+ and the C4MJ have commenced on cell sizes of 1cm^2 and smaller. All of these cells were measured under a High Intensity Pulsed Solar Simulator (HIPSS) using standard production procedures and fully automated test equipment. Testing intensities ranged from 50 W/cm^2 to 81 W/cm^2 depending on customer requirements. HIPSS light sources were calibrated using isotype component cells with calibration traceable to JPL balloon flight cells (in the case of C3MJ+) or to absolute blackbody radiometric standards (in the case of C4MJ). Spectral mismatch calculations were used to generate ASTM G173-03 calibration values for the balloon traceable standards. Several sets of CPV calibration standards were generated; with one set of

standards each being calibrated by Fraunhofer, NREL and AIST. All measurements were done blind.

The initial observed production distributions for the C3MJ+ and C4MJ cell technologies are shown in Fig. 2. Slight differences in typical performance are observed depending on cell size, and whether devices are tested as arrays of cells on-wafer or as discrete die after saw-dicing. The average C3MJ+ performance at 39.3% is fully consistent with previous C3MJ performance and the known improvements associated with reduced series resistance and grid obscuration in the C3MJ+ design. The distribution is based on approximately 2 months of production or > 600,000 cells.

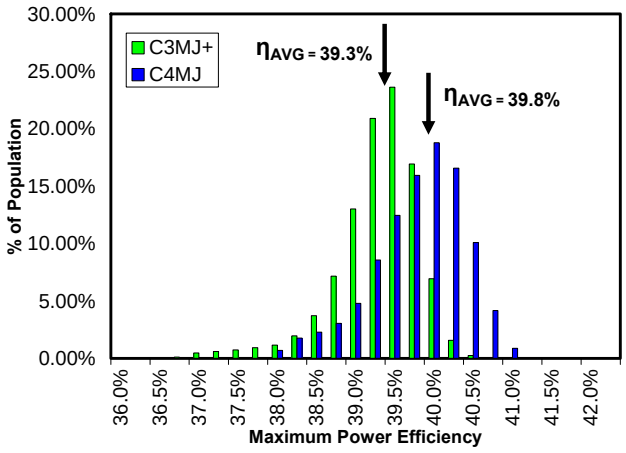

Figure 2. Early production distributions for C3MJ+ (> 600K Cells) and C4MJ (> 16K Cells).

The C4MJ distribution is a preliminary look, based on only four production lots, or about 16,000 cells. The average performance of these first four lots is 39.8%. Prior to entering production, The C4MJ cell technology went through multiple engineering confidence builds over a period greater than a year with mean efficiency greater than 40% for the collection of parts. It is expected that the C4MJ production average will equal or exceed 40% as volume and experience grows.

QUALIFICATION and CHARACTERIZATION

The objective of the C4MJ qualification and characterization (Q&C) program was to enter high volume production with well-characterized device performance and confidence in the reliability of the metamorphic epitaxial structure similar to the confidence that exists in the lattice matched structures that have been in production at Spectrolab for the past 14 years. To achieve this, a qualification test plan was devised to mimic production sampling as much as possible.

The qualification samples were randomly selected from a large population (825 kW rated at 50 W/cm^2) built over six months. Several key processes were intentionally varied to evaluate robustness and stability, and every test was repeated at least twice, to ensure a broad range of process variability was subjected to each test.

Whenever possible, test requirements are derived from a 25 year lifetime under worst case operating conditions for that stress. For example, C4MJ was tested to 1,500 thermal cycles based upon NREL evaluation of the worst case thermal cycle conditions for likely CPV locations [5]. Where 25 year lifetime equivalents are unknown, unprotected cells were tested to or beyond IEC 62108 requirements, but without the protective packaging, encapsulants, and enclosures that are part of the intended configuration for those tests

A partial summary of Q&C test results for the new C4MJ cell technology is described in Table 1. Overall results summarized in **Error! Reference source not found.** show less than 1% degradation in maximum power after all qualification tests

Test	Test Conditions	Results
LIV	25 °C, under 50 W/cm^2 of ASTM G173-03(2008)	Effmp = 39.6%
Temperature and intensity	10, 25, 60, 85 and 110C at 50, 75, 100 and 125 W/cm2	Characterization
Thermal cycle	1,500 cycles from -40C to +110C with 10 min dwells	NPmp = 1.00
Damp heat	85C/85% RH	NPmp=0.990
		NPmp=0.993
Humidity Freeze	500 thermal cycle preconditioning, 20 cycles IEC 62108	NPmp = 0.993
High temperature soak	180, 200, 225 and 250 C in N2	NPmp = 1.00
Accelerated Operating Life	1,000 hrs @ 160°C in air with dark forward current of 0, 1 A & 4 A	NPmp=0.990
ESD	JEDEC CDM 1,000 & 2,000 V	Class IV (Pass 2,000 V)
	JEDEC HBM 4,000 & 8,000 V	Class 3A (Pass 4,000 V)
Outdoor test	> 10 kW on sun for 6 months	No Failures Observed

Table 1. Qualification and characterization tests (partial listing).

Thermal cycle and high temperature soak were two tests of particular interest for the stability of the metamorphic structure. Thermal cycle testing was performed four separate times, with three of the test events completing 1,500 cycles. As indicated in Table 1, average

degradation was less than 0.5% after 1,500 cycles, with the worst case individual degradation less than 2%, which is within measurement error. No cells cracked or broke and no significant changes were seen in electroluminescent images. This indicates metamorphic cells are robust to thermo-mechanical stresses.

C4MJ cells subjected to high temperature soak testing were held at 180˚C, 200˚C, 225˚C and 250˚C. Parts were removed periodically for LIV testing before ultimately accumulating over 2,000 hours. The measured data from each temperature was translated to the maximum operating temperature of 110˚C using an Arrhenius relationship. Fig. 3 shows all the data plotted against the equivalent time at the maximum operating temperature of 110˚C. The model fits the data well and demonstrates that C4MJ is thermally stable well beyond operating life.

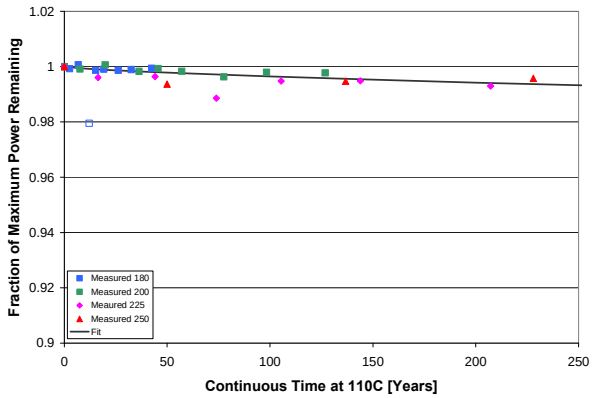

Figure 3. Equivalent lifetime of model, and group average data for cells exposed at four temperatures.

All laboratory tests show C4MJ cells are robust with comparable reliability to previous generations of lattice-matched cells. Even with great lab results, reliability is ultimately determined in the field, and therefore as an additional precaution 10 kW of C4MJ cells completed a six month field trial in an Amonix MegaModule with no detectable degradation prior to completion of qualification.

ON-SUN TESTING

The C4MJ cell technology has entered initial evaluations on-sun in multiple locations in the USA southwest. Amonix has been collecting data on the cumulative energy (MW-h_{AC}) generation in a 7500 series MegaModule® system with C2MJ cell technology on-sun for over two years. With this data, they have developed highly effective models to predict future performance, and have calculated the power generation should C2MJ be replaced by either C3MJ or C4MJ cells. A comparison between the cumulative energy measured with C2MJ cells and predicted energy for C2MJ, C3MJ, and C4MJ cells is shown in Fig. 4. Excellent agreement between measured and predicted values for the C2MJ cell technology validates the effectiveness of the model.

.

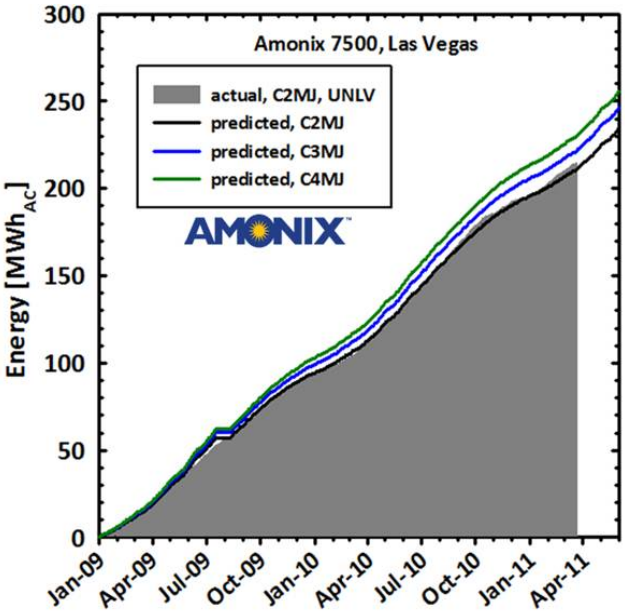

Figure 4. Cumulative energy: measured (C2MJ) and predicted (C2MJ, C3MJ, C4MJ) in Amonix 7500 MegaModule®.

Pre-production C4MJ cells have also been incorporated into the Amonix MegaModule design. A comparison of the daily maximum current generated by each of seven MegaModules located on the same, tracker, but utilizing different cell generations is shown in Fig. 5.

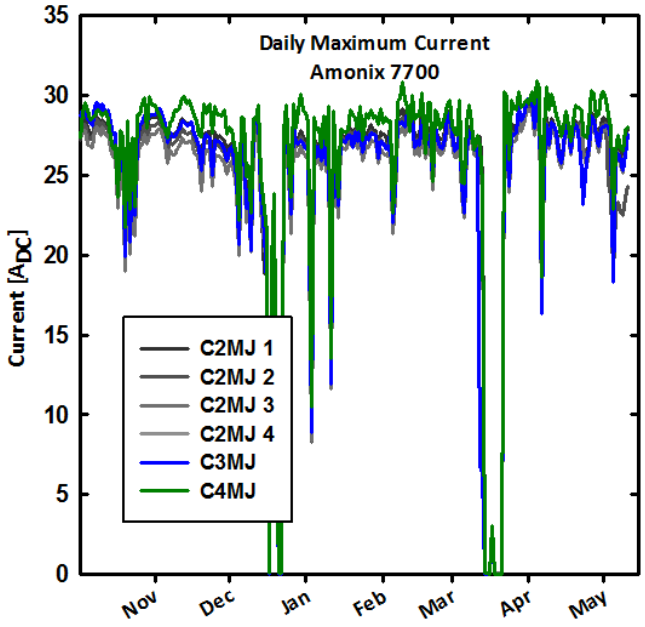

Figure 5. Current generation: measured in Amonix 7700 MegaModule.

Continuous measurements from October 2010 through May 2011 for MegaModules with C2MJ, C3MJ, and C4MJ cell technologies indicate daily and seasonal variation, but do not suggest degradation in performance for any of the cell generations. Each MegaModule contains 1080 individual cell/receiver assemblies.

SPECTRAL RESPONSE OPTIMIZATION

The C4MJ technology affords an opportunity to tailor the cell spectral response to field spectral conditions requiring greater top-cell current density relative to the middle cell current density (the "J-ratio") to a greater extent than was possible in previous lattice-matched cell generations, without performance degradation. Properly applied, this tailoring can provide even greater performance advantages than a direct comparison of AM1.5 efficiency would suggest.

The ASTM G173 direct spectrum was originally formulated to provide a good composite representation of spectral conditions on clear, sunny days in the US southwest [6-8]. However, recently Kinsey [9] and others [10] have performed detailed annual analyses of energy yield at US southwest sites and shown that cells optimized for the ASTM spectrum are not optimal for maximizing total energy yield. These studies suggest that a design with a greater top cell current density (higher J-ratio) would result in higher overall energy production.

In order to assess the optimal J-ratio we performed a generalized analysis for several US sites and included the effects of modifications of the incident solar spectrum on the cell due to real optical transmittance functions supplied by multiple CPV module manufacturers. The deviation of optimum J-ratio from the J-ratio implied by the ASTM spectrum is thus subdivided into site-dependent and optics-dependent components.

The site dependence was addressed by constructing a composite spectrum at each site using a combination of hourly data supplied by TMY3 Typical Meteorological Year files supplied by the National Renewable Energy Laboratory [10] and spectral modeling of the direct normal irradiance at each hour using the SMARTS solar radiation model [11]. The climatic data for each hour in the subject TMY3 site file was used to generate a SMARTS run to produce detailed hourly spectra. All spectra were integrated and then normalized to the DNI reported in the TMY3 data set for the given hour. The composite spectrum for a given site then was constructed by calculating the average spectral intensity at each wavelength, weighted by the integrated DNI in the spectral range from 350–950 nm (the approximate wavelength range of response by the top and middle cell), i.e.

$$\mathrm{DNI}(\lambda) = \frac{\sum_{t=\text{all daylight hours}} \mathrm{DNI}(\lambda,t)\int_{350\mathrm{nm}}^{950\mathrm{nm}} \mathrm{DNI}(\lambda,t)d\lambda}{\sum_{t=\text{all daylight hours}} \int_{350\mathrm{nm}}^{950\mathrm{nm}} \mathrm{DNI}(\lambda,t)d\lambda}$$

The spectral values are thus weighted by their energy-producing potential by a cell whose current is limited by the top or middle cell. We excluded hours in which the sun elevation was less than 5° above the horizon since at such low angles the majority of the collector is typically shaded. The resulting composite spectra are shown in Fig. 6. In addition to southwestern sites, Tampa has been included to provide a high humidity atmospheric case.

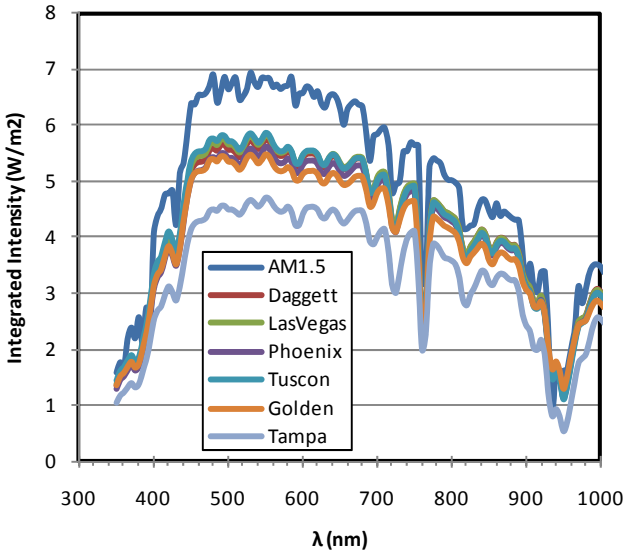

Figure 6. Composite spectra at several US sites.

Fig. 7 shows the calculated J-ratio difference for each of these sites considering spectrum only (no optics) for the cell at room temperature (typical cell test condition) and at 60°C, a typical nominal cell operating temperature in the field. Temperature dependence is due to the bandgap shifts of both the top and middle cell (and corresponding cutoff wavelength shifts), which was modeled from an initial room temperature quantum efficiency measurement of a cell with J-ratio=1 and the known temperature coefficients as previously described by Kinsey and Edmondson [12]. The vertical axis is the surplus or deficit in J-ratio that would result at the given site and temperature for a cell that has J-ratio=1.0 under the ASTM spectrum at 21°C (so for example, the Daggett composite spectrum would result in a deficit of 4.8% or a J-ratio of 95.2% for a cell at room temperature

Fig. 8 shows the effect of typical acrylic optics on the J-ratio, again by comparison with a cell having J-ratio = 1.0 under the ASTM spectrum at 21°C. The vertical axis interpretation is the same as for Fig. 7. The transmittances used are those reported by Miller et al in a comprehensive study of PMMA field performance [13]. The J-ratio deficit due to new PMMA is ~1.5%, and aging adds another

~0.9%. Notice also that soiling adds another deficit of ~6% (for heavy soiling), and this can be expected to apply to any CPV system, not just those with PMMA.

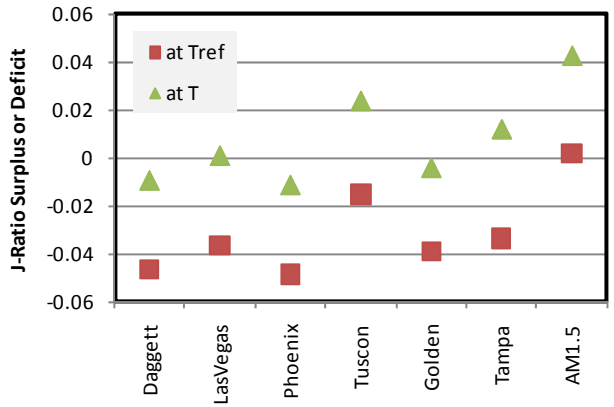

Figure 7. J-ratio surplus/deficit at multiple sites based on their composite spectra (relative to J-ratio=1.0 for the ASTM spectrum) (T_{REF}=21˚C, T=60˚C).

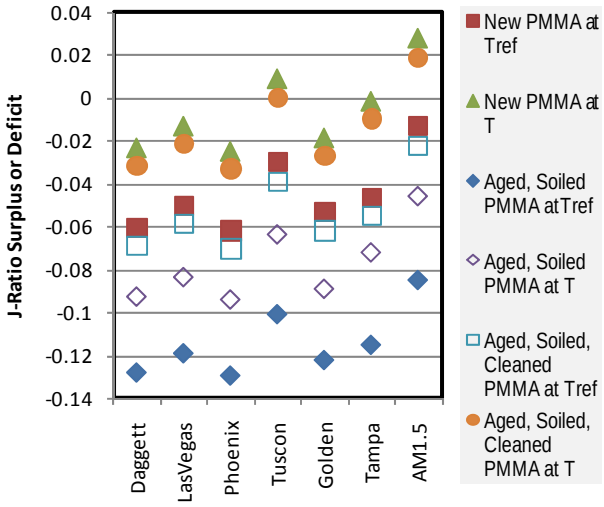

Figure 8. Impact of PMMA lenses with aging and soiling on J-ratio (T_{REF}=21˚C, T=60˚C).

Fig. 9 compares the spectral effect of system optical transmittance for a wide variety of CPV systems. All of these data points are J-ratios using the ASTM spectrum as a baseline, and it can be seen that there is a spread of ~5% in J-ratio across all the systems.

Considering all of these observations, it is clear that there is a spread in optimum J-ratio both across sites and across system designs. Although this is an approximate analysis (for example, variation of cell temperature with DNI or wind speed has not been accounted for), it appears likely that a J-ratio slightly greater than 1.0 (referenced to the ASTM spectrum) will produce maximum energy output. For deployment sites of sufficient size, it is economical to tailor a J-ratio which is specific to the site and system design.

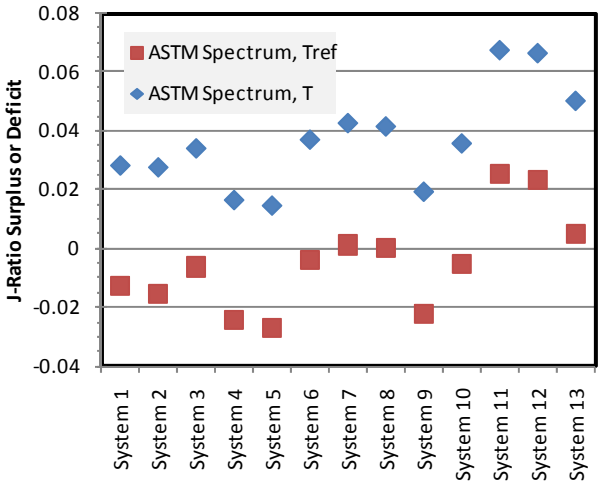

Figure 9. Impact of system optical transmittance on J-ratio for a variety of CPV systems (T_{REF}=21˚C, T=60˚C).

.

CONCLUSION

Both the research record efficiencies and practical production efficiencies of multijunction cells continue to evolve rapidly. The latest generation of lattice-matched cells now achieves 39.3% average efficiency in volume production. A new generation of metamorphic cells has now begun production, and represents two milestones for the CPV industry: the first production cell employing a metamorphic epitaxial structure and the first cell in volume production expected to achieve 40% average efficiency. Extensive qualification tests have shown that the new metamorphic structure has the same high reliability as its lattice-matched predecessors, opening new vistas for continuing advances in the efficiency of multijunction cells. The metamorphic cell design also affords a wider range of bandgap tailoring possibilities to optimize performance for specific sites and module designs.

ACKNOWLEDGEMENTS

The authors would like to thank the entire R&D and production engineering teams at Spectrolab and Amonix. Support from the US DOE under the Technology Pathway Partnership program is gratefully acknowledged.

This work was partially funded by the U.S. Department of Energy under the Solar Energy Technologies Program, Contract .No. DE-FC3607GO17052.

REFERENCES

[1] Diandra Weldon (April 14, 2011) *Solar Junction Breaks World Record with 43.5% Efficient CPV Production Cell,* press release, retrieved April 14, 2011,

http://www.sjsolar.com/downloads/Solar_Junction_World Record_%20Efficiency_14April11.pdf

[2] R.K. Jones et al., "Status of 40% Production Efficiency Concentrator Cells at Spectrolab," *IEEE 35th Photovoltaics Specialists Conference*, Honolulu, Hawaii, 2010.

[3] R. R. King et al., "Band Gap-Voltage Offset and Energy Production in Next-Generation Multijunction Solar Cells," *Proceedings of the 25th European PV Solar Energy Conference,"* Valencia, Spain, 2010.

[4] C. Fetzer et al., "MOVPE Development of III/V Multijunction CPV at Spectrolab," *International Conference on Concentrating Photovoltaic Systems (CPV-6)*, Freiburg, Germany, 2010.

[5] N. Bosco and S. Kurtz, "Quantifying the Thermal Fatigue of CPV Modules," *International Conference on Concentrating Photovoltaic Systems (CPV-6)*, Freiburg, Germany, 2010.

[6] Myers, Emery and Gueymard, "Proposed Reference Spectral Irradiance Standards to Improve Concentrating Photovoltaic System Design and Performance Evaluation," Proc. IEEE PVSC 2002 p. 923.

[7] Emery, Myers, and Kurtz, "What is the Appropriate Reference Spectrum for Characterizing Concentrator Solar Cells?", Proc. IEEE PVSC, 2002, p. 840.

[8] McMahon, Kurtz, Emory, and Young, "Criteria for the Design of GaInP/GaAs/Ge Triple-Junction Cells to Optimize Their Performance Outdoors," Proc. IEEE PVSC, 2002, p. 931.

[9] Kinsey, "More power, more energy in Amonix solar power plants," CPV-7, Las Vegas, NV, April 2011.

[10] Wilcox and Marion, *Users Manual for TMY3 Data Sets*, National Renewable Energy Laboratory Technical Report NREL/TP-581-43156, Revised May 2008

[11] Gueymard. "Parameterized transmittance model for direct beam and circumsolar spectral irradiance.", *Solar Energy* , 71(5):325–346, 2001.

[12] Kinsey and Edmondson, "Spectral Response and Energy Output of Concentrator Multijunction Solar Cells," Progress in Photovoltaics: Research and Applications, Wiley, 2008.

[13] Miller et al, "Durability of Poly(Methyl Methacrylate) Lenses Used in Concentrating Photovoltaic Modules," Proc. of SPIE Vol. 7773 777303-1.